Low-energy electron holographic imaging of individual tobacco mosaic virions

Longchamp, Jean-Nicolas ; Latychevskaia, Tatiana ; Escher, Conrad ; Fink, Hans-Werner

Abstract: Modern structural biology relies on Nuclear Magnetic Resonance (NMR), X-ray crystallography, and cryo-electron microscopy for gaining information on biomolecules at nanometer, sub-nanometer, or atomic resolution. All these methods, however, require averaging over a vast ensemble of entities, and hence knowledge on the conformational landscape of an individual particle is lost. Unfortunately, there are now strong indications that even X-ray free electron lasers will not be able to image individual molecules but will require nanocrystal samples. Here, we show that non-destructive structural biology of single particles has now become possible by means of low-energy electron holography. As an example, individual tobacco mosaic virions deposited on ultraclean freestanding graphene are imaged at 1 nm resolution revealing structural details arising from the helical arrangement of the outer protein shell of the virus. Since low-energy electron holography is a lens-less technique and since electrons with a deBroglie wavelength of approximately 1 Å do not impose radiation damage to biomolecules, the method has the potential for Angstrom resolution imaging of single biomolecules.

DOI: https://doi.org/10.1063/1.4931607

AIP | Applied Physics Letters

Low-energy electron holographic imaging of individual tobacco mosaic virions

Jean-Nicolas Longchamp, Tatiana Latychevskaia, Conrad Escher, and Hans-Werner Fink

Citation: Applied Physics Letters **107**, 133101 (2015); doi: 10.1063/1.4931607
View online: http://dx.doi.org/10.1063/1.4931607
View Table of Contents: http://scitation.aip.org/content/aip/journal/apl/107/13?ver=pdfcov
Published by the AIP Publishing

Low-energy electron holographic imaging of individual tobacco mosaic virions

Jean-Nicolas Longchamp,[a] Tatiana Latychevskaia, Conrad Escher, and Hans-Werner Fink
Physics Department, University of Zurich, Winterthurerstrasse 190, 8057 Zurich, Switzerland

(Received 2 July 2015; accepted 7 August 2015; published online 28 September 2015)

Modern structural biology relies on Nuclear Magnetic Resonance (NMR), X-ray crystallography, and cryo-electron microscopy for gaining information on biomolecules at nanometer, sub-nanometer, or atomic resolution. All these methods, however, require averaging over a vast ensemble of entities, and hence knowledge on the conformational landscape of an individual particle is lost. Unfortunately, there are now strong indications that even X-ray free electron lasers will not be able to image individual molecules but will require nanocrystal samples. Here, we show that non-destructive structural biology of single particles has now become possible by means of low-energy electron holography. As an example, individual tobacco mosaic virions deposited on ultraclean freestanding graphene are imaged at 1 nm resolution revealing structural details arising from the helical arrangement of the outer protein shell of the virus. Since low-energy electron holography is a lensless technique and since electrons with a deBroglie wavelength of approximately 1 Å do not impose radiation damage to biomolecules, the method has the potential for Angstrom resolution imaging of single biomolecules. © *2015 AIP Publishing LLC*. [http://dx.doi.org/10.1063/1.4931607]

Structural information about biomolecules at nanometer, sub-nanometer, or atomic resolution is nowadays predominantly obtained by X-ray crystallography and NMR spectroscopy, whereby samples in the form of crystals or in liquids are studied. This, however, entails important structural information being averaged over many molecules. Thus, relevant details in molecules exhibiting diverse structural conformations remain undiscovered. Besides this drawback, these methods can only be applied to a limited subset of biological molecules that either readily crystallize for use in X-ray studies or are small enough for NMR investigations. A third approach towards imaging single particles is cryo-electron microscopy; however, for biological samples, the possible resolution is limited by radiation damage caused by the high electron energy employed in conventional transmission electron microscopes (TEMs).[1] Due to the strong inelastic scattering of high-energy electrons, there is little hope for obtaining structural information at atomic resolution for a single entity. As the permissible dose is limited to $10\,e^{-}/Å^2$ only, an individual molecule is destroyed long before an image of high enough quality could be acquired.[2,3] The radiation damage problem is usually circumvented by averaging over several thousand noisy images in order to attain a satisfactory signal-to-noise ratio.[4] The alignment and averaging routines inherent to high-resolution cryo-electron microscopy limit its application range to symmetric and particularly rigid objects, such as specific classes of viruses. Despite the shortcomings of the three conventional structural biology tools discussed above, one needs to express respect for the vast amount of data that has been generated over the past decades, reflected by the impressive volume of the current protein database.

Nevertheless, a milestone for structural biology would definitely be attained if methods and tools were available, that do away with averaging over an ensemble of molecules and enable structural biology on a truly single molecule level. To obtain atomic resolution information about the structure of any individual biological molecule, different concepts and technologies are needed. One approach of this kind is associated with the recent X-ray free electron laser (XFEL) projects. This approach initially appeared to be a promising method for gaining information from just one single biomolecule at the atomic scale by recording its X-ray diffraction pattern within the short time of just 10 fs, before the molecule is decomposed by radiation damage. Unfortunately, there are now strong indications[5] that again averaging over a large number of molecules is inevitable in order to obtain images with a sufficiently high signal-to-noise ratio enabling numerical reconstruction of the diffraction pattern with atomic resolution.[6–8]

The approach to structural biology at the single particle level described here is motivated by the experimental evidence that low-energy electrons with a kinetic energy in the range of 50–250 eV are harmless to biomolecules.[9–11] Even after exposing fragile molecules like DNA or proteins to a total electron dose of $10^6\,e^{-}/Å^2$, i.e., more than five orders of magnitude higher than the critical dose in TEM, no radiation damage could be observed. This, combined with the fact that the deBroglie wavelengths associated with this energy range are between 0.7 and 1.7 Å, makes low-energy electron microscopy an auspicious candidate for structural biology at the single molecule level.[11,12] During the last three decades, DNA, phages, viruses, and individual ferritin proteins attached to carbon nanotubes were imaged by means of low-energy electron holography with nanometer resolution.[9,10,13–15] For imaging, the objects of interest used to be placed across bores in a membrane. Unfortunately, after such preparation, the holographic record often suffered from

[a]Author to whom correspondence should be addressed. Electronic mail: longchamp@physik.uzh.ch

biprism distortion limiting the resolution in the reconstruction.[16] This artifact is suppressed if the specimen is placed on an electrically conductive substrate with sufficient transparency for low-energy electrons.[17–19] Yet, the substrate has to be robust enough to withstand the deposition procedure.[20] It turned out that freestanding graphene, an atomically thin layer of carbon atoms arranged in a honeycomb lattice, fulfills all these requirements. Electron transmission measurements have shown that more than 70% of the low-energy electrons are transmitted through graphene and therefore are available for imaging objects deposited on the two dimensional substrate.[18]

Tobacco mosaic virus (TMV) is a rod-shaped virus, approximately 300 nm in length and 18 nm in diameter, discovered at the end of the 19th century.[21–24] The first molecular model of TMV at atomic resolution was obtained from X-ray fiber diffraction experiments by Namba *et al.* in 1986.[25,26] Retrieving information about unstained TMV at the sub-nanometer scale is possible by means of cryo-electron microscopy since the 1980s.[27,28] The most recent models that can be found in the protein database are either obtained from X-ray fiber diffraction data (2.9 Å resolution) or high-energy transmission electron microscopy investigations (5 Å resolution). In both cases, the Angstrom resolution could only be obtained by averaging over a vast number of entities.

Here, we show that, by means of low-energy electron holography, it is possible to image individual TMVs deposited on ultraclean freestanding graphene. The virions are imaged with 1 nm resolution exhibiting details of the helical TMV structure.

In our low-energy electron holographic setup (Fig. 1(a)), inspired by Gabor's original idea of in-line holography,[29–31] a sharp (111)-oriented tungsten tip (Fig. 1(b)) acts as source of a divergent beam of highly coherent electrons.[31–34] The electron field emitter can be brought as close as 100 nm to the sample with the help of a 3-axis nanopositioner. Part of the electron wave is elastically scattered off the object and hence is called the object wave, while the un-scattered part of the wave represents the reference wave. At a distant detector, the hologram, i.e., the pattern resulting from the interference of these two waves is recorded. The magnification of the imaging system is given by the ratio between detector-to-source distance and sample-to-source distance and can be as high as 10^6. A hologram, in contrast to a diffraction pattern, contains the phase information of the object wave, and the object structure can thus be reconstructed unambiguously. The numerical reconstruction from the hologram is essentially achieved by back propagation to the object plane, which corresponds to evaluating the Fresnel-Kirchhoff integral transformation.[35–40] In low-energy electron holography, a lens-less technique not suffering from lens aberrations, the resolution limit is given by the deBroglie wavelengths (λ) and by the numerical aperture (NA) of the detector system. With λ being as small as 0.7 Å and NA = 0.54, Angstrom and even atomic resolution shall eventually be possible.

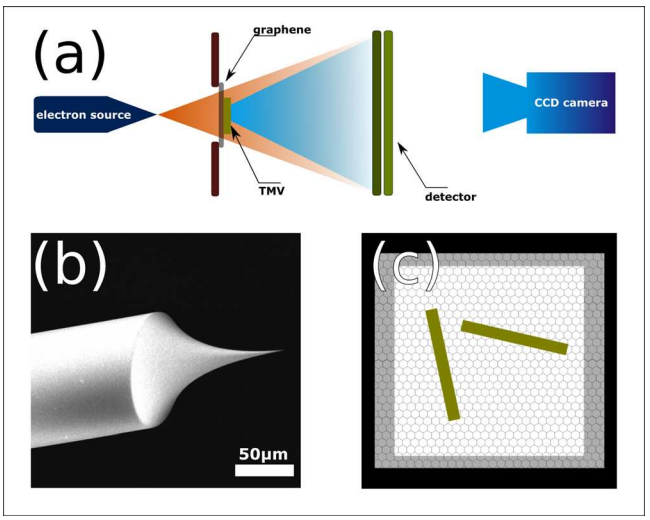

FIG. 1. Illustration of the experimental scheme for low-energy electron holography. (a) The source-to-sample distance amounts to typically 100–1000 nm which leads to kinetic electron energies in the range of 50–250 eV and the sample-to-detector distance is 70 mm. With an electron detector of 75 mm in diameter, an acceptance angle of 56° is achieved (full angle). (b) SEM image of an electrochemically etched W(111) tip acting as field-emitter of a divergent coherent low-energy electron beam. (c) Schematic illustration of the sample geometry with two TMVs lying on ultraclean freestanding graphene suspended over a square aperture.

Ultraclean freestanding graphene, covering ion milled square-like apertures of approximately 500 nm side length, is prepared by the platinum-metal catalysis method, described in detail recently elsewhere.[41] This method leads to large atomically clean areas, up to several square microns in size.[19] In Fig. 2(a), a low-energy electron transmission image of ultraclean freestanding graphene layer is presented. Transmission measurements have shown that single layer graphene exhibits a transparency of more than 70% for low-energy electrons.[18] Figs. 2(b) and 2(c) display low-energy electron holograms recorded at kinetic energies of 131 eV and 125 eV, respectively. In these images, the rod-like virions deposited on graphene are apparent besides traces of contaminations resulting from the sample preparation procedure. Nevertheless, the cleanliness of the graphene is maintained throughout the entire preparation process to a sufficient level for imaging. A detailed description of the preparation and deposition method of TMV on graphene can be found in the supplementary material.[42]

In Figs. 3(a) and 3(c), two high magnification holograms of TMV are displayed. From these holograms, the shape of the corresponding virions is reconstructed at 1 nm resolution (see Figs. 3(b) and 3(d)). The diameter of the virion corresponds to 18 nm as expected. Furthermore, one can observe, as emphasized by yellow arrows in Fig. 3(b), apex-like features on the rim of the virion, which we attribute to the helical arrangement of the outer protein shell of TMV. The spatial resolution attained in a hologram can be estimated using the Abbe criterion[43,44] and by measuring the largest angle under which interference fringes are observable.[39,40,45] This is illustrated in Fig. 4(b), where an intensity profile along the blue line in the hologram is displayed. The highest order interference fringe observed in the hologram is found at a scattering angle of 88 mrad. Given the electron wavelength of 1.37 Å for an electron kinetic energy of 80 eV, this angle corresponds to a spatial resolution of approximately 0.8 nm.

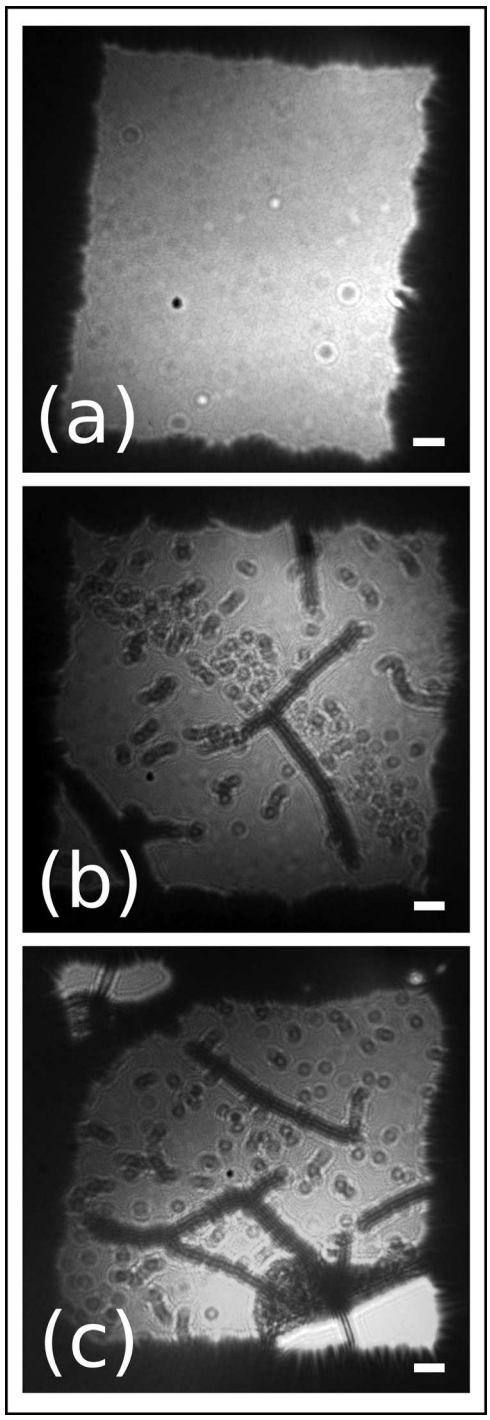

FIG. 2. Low-energy electron holograms before and after TMV deposition on ultraclean freestanding graphene. (a) Freestanding graphene covering a square aperture milled in a Pd-coated SiN membrane. Before TMV deposition, the graphene layer is ultraclean. (b) and (c) Low-energy electron holograms of TMVs deposited onto freestanding graphene. The scale bar corresponds to 50 nm.

Electrons with a kinetic energy of 80 eV and 89 eV exhibit deBroglie wavelengths of 1.37 Å and 1.29 Å, respectively. This combined with the fact that in low-energy electron holography the resolution is neither limited by lens aberrations nor by radiation damage, Angstrom or even atomic resolution may be expected. The nanometer resolution that we report here has to be attributed to residual mechanical vibrations. In a low-energy electron hologram, the spacing between consecutive interference fringes gradually

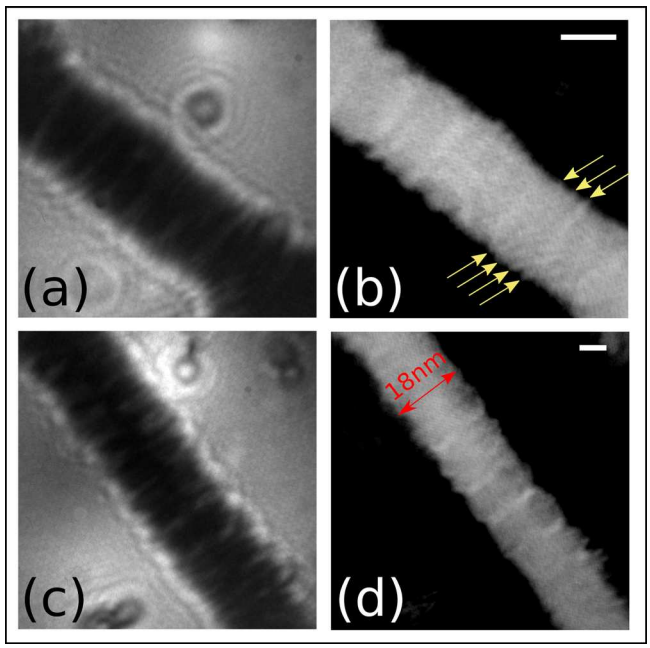

FIG. 3. High-magnification holograms of TMV and the respective reconstructions. (a) and (c) Holograms of TMV recorded with 80 eV, respectively, 89 eV electron energy. (b) and (d) Reconstructed TMV images from (a) and (c) (inverted gray scale). Yellow arrows emphasize in (b) the presence of apex-like features on the rim of the TMV. These details are attributed to the helical structure of the virus. The scale bar corresponds to 10 nm.

decreases towards higher orders. Hence, high-order interference fringes and consequently high-resolution structural details are most susceptible to mechanical vibrations.

Even if the current resolution is of the order of 1 nm, one can already compare the images obtained with low-energy electrons with an atomic TMV model constructed by Sgro[46] with the atomic coordinates available from the protein database (pdb id: 2tmv) (Fig. 5(a)). Figs. 5(b) and 5(c) are close-ups of the TMV images displayed in Fig. 3. Once the atomic TMV model is superimposed to match the width of the viruses (see Figs. 5(e) and 5(f)), the apex-like features that we previously attributed to the helical structure of the virus are now coinciding with the peaks of the helical structure in the model. The agreement between model and experimental data obtained from a single particle is remarkable. To take into account the kink in the TMV shown in Fig. 5(e), two copies of the model, rotated by 6° with respect to each other, are superimposed on the low-energy electron images. By this, further details, marked by yellow arrows in Fig. 5(b), which correspond to the helical structure of the virus are now congruent with the atomic model. In Fig. 5(d), an intensity plot along the blue line present in Fig. 5(b) is displayed. The distance between depletions in this graph corresponds to approximately 2.35–2.40 nm, a length that almost perfectly fits the expected 2.30 nm helical pitch from X-ray fiber diffraction investigations.[47,48] The spatial resolution in the reconstructed TMV structure can be estimated by measuring the edge response.[49] The apex like features of the TMV structure represent an edge on which such a measurement can be done. By applying the common 10%–90% limits (not shown here) on the intensity line scan in Fig. 5(d), a resolution of 0.95 nm is obtained, in good agreement with the interference resolution criterion discussed above.

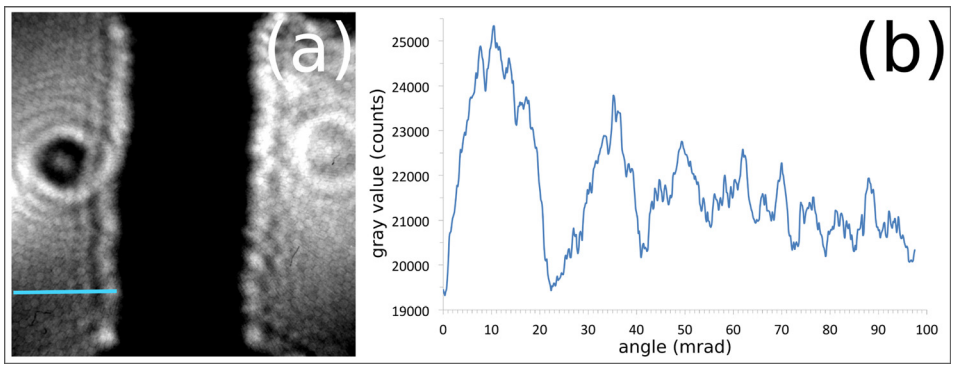

FIG. 4. Illustration of the resolution in a low-energy electron hologram of TMV. (a) 80 eV hologram of TMV presented in Fig. 3(a) but rotated and with enhanced contrast to reveal higher-order interference fringes. The hexagonal pattern observed in this image is due to the geometrical arrangement of the channels in the MCP-detector. (b) Intensity scan along the blue line in (a). Interference fringes can be observed up to an angle of 88mrad. With a wavelength of 1.37 Å, associated to 80 eV electrons, this angle corresponds to a resolution of 0.8 nm. The modulations due to the presence of the multichannel plate channels are much lower than the signal obtained from the interference fringes of the hologram.

A further observation in Figs. 5(b) and 5(c) is the presence of bright stripes across the virus separated by 7 nm. While these bright stripes correspond to higher material density, we do not understand the underlying biological origin. Nevertheless, we would like to hint that the observed 7 nm distance is very close to the literature value of 6.9 nm associated with the thickness of a TMV subunit.[48,50] Similar features have been observed in TEM investigations of uranyl acetate stained *in-vitro* assembled viruses[51,52] but, to our knowledge, never on *in-vivo* purified TMV.

In this letter, we report the first nanometer resolved images of single tobacco mosaic virions obtained from low-energy electron investigations. Details revealed on the rim of the TMV are attributed to the helical structure of the virus by confronting our images with an atomic model based on the coordinates available from the protein database. With this,

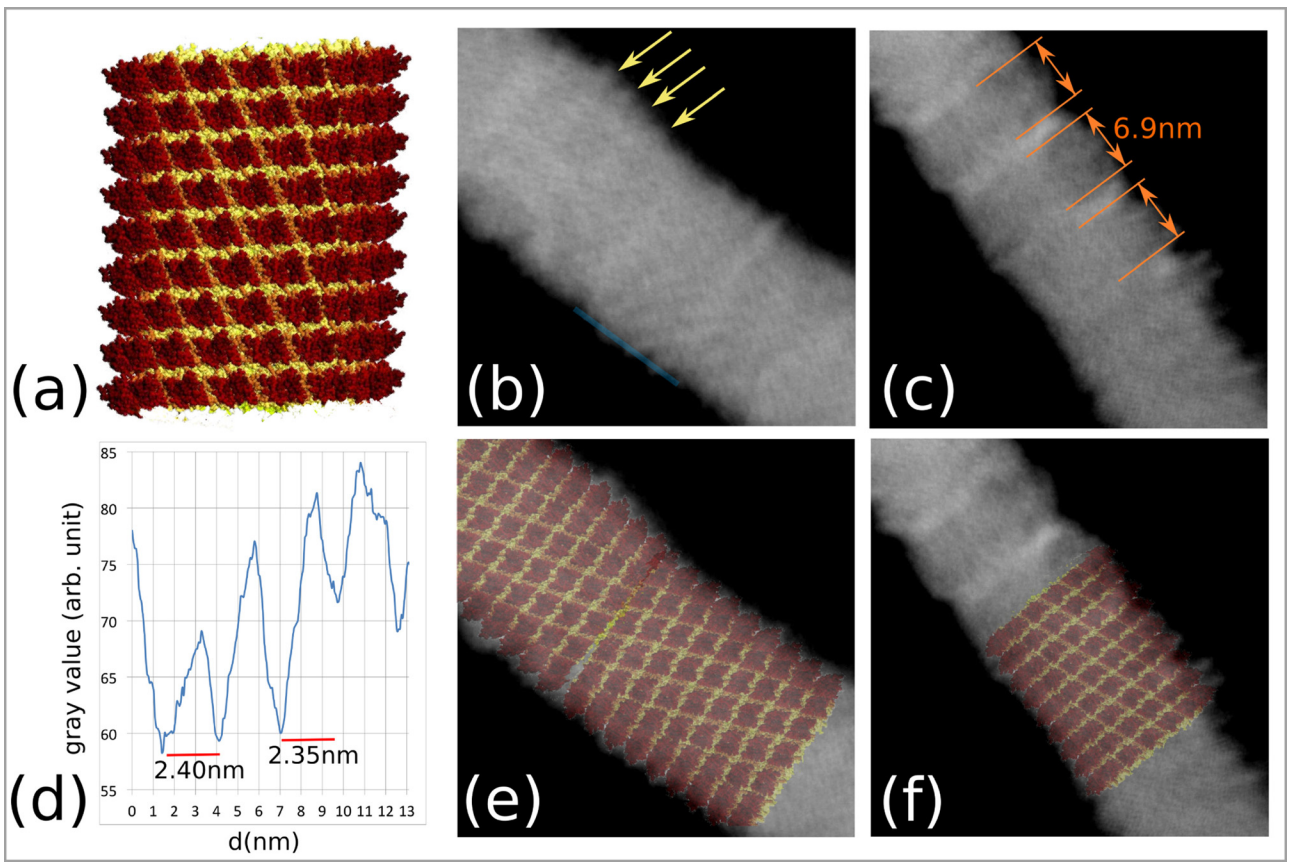

FIG. 5. Comparison of an atomic TMV model with the low-energy electron images. (a) Atomic TMV model constructed from the coordinates available from the protein database (pdb id: 2tmv). (b) and (c) Close-ups of the reconstructed TMV images presented in Fig. 3. In (b), yellow arrows mark further apex-like features coinciding with the atomic model. In (c), the distance between bright stripes is emphasized and marked according to the literature value of 6.9 nm for the thickness of a subunit. (d) Intensity scan along the blue line in (b). (e) and (f) Atomic TMV model superimposed on the same images as in (b) and (c). From Sgro, *Virus Taxonomy: VIIIth Report of the International Committee on Taxonomy of Viruses*, 1st Edition, edited by C. M. Fauquet, M. A. Mayo, J. Maniloff, U. Desselberger, and L. A. Ball. Copyright 2005 Academic Press. Reproduced with permission from Academic Press.

we have demonstrated the potential of low-energy electron holography for structural biology at the single particle level.

The current nanometer resolution will be pushed to Angstrom resolution in the near future by improving the mechanical stability of the microscope. Furthermore, we have recently reported that by employing a slightly modified experimental setup, where a parallel beam of low-energy electrons is illuminating the sample, we could image a region of 210 nm in diameter of freestanding graphene with 2 Å resolution.[53] This experimental scheme will now also be used to image TMV at similar resolution.

The authors are grateful for financial support by the Swiss National Science Foundation (Grant No. PZ00P2 148084). We would like to thank Annette Niehl and Manfred Heinlein from the CNRS Strasbourg for the TMV purification and helpful discussions. We also would like to thank Kishan Thodkar and Christian Schönenberger from the University of Basel for providing us with their CVD grown graphene.

[1]R. Henderson, Q. Rev. Biophys. **28**, 171 (1995).
[2]E. Knapek and J. Dubochet, J. Mol. Biol. **141**, 147 (1980).
[3]R. F. Egerton, P. Li, and M. Malac, Micron **35**, 399 (2004).
[4]M. van Heel, B. Gowen, R. Matadeen, E. V. Orlova, R. Finn, T. Pape, D. Cohen, H. Stark, R. Schmidt, M. Schatz, and A. Patwardhan, Q. Rev. Biophys. **33**, 307 (2000).
[5]J. W. Miao, H. N. Chapman, J. Kirz, D. Sayre, and K. O. Hodgson, Annu. Rev. Biophys. Biomol. Struct. **33**, 157 (2004).
[6]R. Neutze, R. Wouts, D. van der Spoel, E. Weckert, and J. Hajdu, Nature **406**, 752 (2000).
[7]V. L. Shneerson, A. Ourmazd, and D. K. Saldin, Acta Crystallogr., Sect. A **64**, 303 (2008).
[8]H. N. Chapman, P. Fromme, A. Barty, T. A. White, R. A. Kirian, A. Aquila, M. S. Hunter, J. Schulz, D. P. DePonte, U. Weierstall, R. B. Doak, F. R. N. C. Maia, A. V. Martin, I. Schlichting, L. Lomb, N. Coppola, R. L. Shoeman, S. W. Epp, R. Hartmann, D. Rolles, A. Rudenko, L. Foucar, N. Kimmel, G. Weidenspointner, P. Holl, M. Liang, M. Barthelmess, C. Caleman, S. Boutet, M. J. Bogan, J. Krzywinski, C. Bostedt, S. Bajt, L. Gumprecht, B. Rudek, B. Erk, C. Schmidt, A. Homke, C. Reich, D. Pietschner, L. Struder, G. Hauser, H. Gorke, J. Ullrich, S. Herrmann, G. Schaller, F. Schopper, H. Soltau, K.-U. Kuhnel, M. Messerschmidt, J. D. Bozek, S. P. Hau-Riege, M. Frank, C. Y. Hampton, R. G. Sierra, D. Starodub, G. J. Williams, J. Hajdu, N. Timneanu, M. M. Seibert, J. Andreasson, A. Rocker, O. Jonsson, M. Svenda, S. Stern, K. Nass, R. Andritschke, C.-D. Schroter, F. Krasniqi, M. Bott, K. E. Schmidt, X. Wang, I. Grotjohann, J. M. Holton, T. R. M. Barends, R. Neutze, S. Marchesini, R. Fromme, S. Schorb, D. Rupp, M. Adolph, T. Gorkhover, I. Andersson, H. Hirsemann, G. Potdevin, H. Graafsma, B. Nilsson, and J. C. H. Spence, Nature **470**, 73 (2011).
[9]M. Germann, T. Latychevskaia, C. Escher, and H.-W. Fink, Phys. Rev. Lett. **104**, 095501 (2010).
[10]J.-N. Longchamp, T. Latychevskaia, C. Escher, and H.-W. Fink, Appl. Phys. Lett. **101**, 93701 (2012).
[11]T. Latychevskaia, J.-N. Longchamp, C. Escher, and H.-W. Fink, "Holography and coherent diffraction with low-energy electrons: A route towards structural biology at the single molecule level," Ultramicroscopy (to be published).
[12]L. Livadaru, J. Mutus, and R. A. Wolkow, J. Appl. Phys. **110**, 094305 (2011).
[13]H.-W. Fink, H. Schmid, E. Ermantraut, and T. Schulz, J. Opt. Soc. Am. A **14**, 2168 (1997).
[14]P. Simon, H. Lichte, P. Formanek, M. Lehmann, R. Huhle, W. Carrillo-Cabrera, A. Harscher, and H. Ehrlich, Micron **39**, 229 (2008).
[15]G. B. Stevens, M. Krüger, T. Latychevskaia, P. Lindner, A. Plückthun, and H.-W. Fink, Eur. Biophys. J. **40**, 1197 (2011).
[16]T. Latychevskaia, J.-N. Longchamp, C. Escher, and H.-W. Fink, Ultramicroscopy **145**, 22–27 (2014).
[17]J. Y. Mutus, L. Livadaru, J. T. Robinson, R. Urban, M. H. Salomons, M. Cloutier, and R. A. Wolkow, New J. Phys. **13**, 63011 (2011).
[18]J.-N. Longchamp, T. Latychevskaia, C. Escher, and H.-W. Fink, Appl. Phys. Lett. **101**, 113117 (2012).
[19]J.-N. Longchamp, C. Escher, T. Latychevskaia, and H.-W. Fink, Ultramicroscopy **145**, 80–84 (2014).
[20]R. R. Nair, P. Blake, J. R. Blake, R. Zan, S. Anissimova, U. Bangert, A. P. Golovanov, S. V. Morozov, A. K. Geim, K. S. Novoselov, and T. Latychevskaia, Appl. Phys. Lett. **97**, 153102 (2010).
[21]D. Ivanowski, St.-Petersbourg. "Concerning the mosaic disease of the tobacco plant. Trans. J. Johnson," in *Phytopathological Classics Number 7*. (American Phytopathological Society, St. Paul, MN, 1892) pp. 27–30.
[22]E. F. Smith, J. Mycol. **7**, 382 (1894).
[23]M. W. Beijerinck, "Concerning a contagium vivum fluidum as cause of the spot disease of tobacco leaves," in *Phytopathological Classics*, No. 7 (American Phytopathological Society, St. Paul, MN., 1898).
[24]A. Lustig and A. J. Levine, J. Virol. **66**, 4629 (1992).
[25]K. Namba and G. Stubbs, Science **231**, 1401 (1986).
[26]K. Namba, R. Pattanayek, and G. Stubbs, J. Mol. Biol. **208**, 307 (1989).
[27]T.-W. Jeng, R. A. Crowther, G. Stubbs, and W. Chiu, J. Mol. Biol. **205**, 251 (1989).
[28]C. Sachse, J. Z. Chen, P.-D. Coureux, M. E. Stroupe, M. Fändrich, and N. Grigorieff, J. Mol. Biol. **371**, 812 (2007).
[29]D. Gabor, Nature **161**, 777 (1948).
[30]D. Gabor, *Noble Lecture in Physics 1971-1980,* (World Scientific Publishing Co., Pte. Ltd., Singapore, 1992).
[31]H.-W. Fink, W. Stocker, and H. Schmid, Phys. Rev. Lett. **65**, 1204 (1990).
[32]H. W. Fink, IBM J. Res. Dev. **30**, 460 (1986).
[33]H. W. Fink, W. Stocker, and H. Schmid, J. Vac. Sci. Technol., B **8**, 1323 (1990).
[34]H. W. Fink, Ultramicroscopy **50**, 101 (1993).
[35]H. J. Kreuzer, K. Nakamura, A. Wierzbicki, H. W. Fink, and H. Schmid, Ultramicroscopy **45**, 381 (1992).
[36]H. J. Kreuzer, Micron **26**, 503 (1995).
[37]T. Latychevskaia and H.-W. Fink, Phys. Rev. Lett. **98**, 233901 (2007).
[38]T. Latychevskaia and H.-W. Fink, Opt. Express **17**, 10697 (2009).
[39]T. Latychevskaia, J.-N. Longchamp, and H.-W. Fink, Opt. Express **20**, 28871 (2012).
[40]T. Latychevskaia and H.-W. Fink, Appl. Opt. **54**, 2424 (2015).
[41]J.-N. Longchamp, C. Escher, and H.-W. Fink, J. Vac. Sci. Technol., B: Microelectron. Nanometer Struct. **31**, 020605 (2013).
[42]See supplementary material at http://dx.doi.org/10.1063/1.4931607 for a detailed description of the preparation and deposition method of TMV on graphene.
[43]E. Abbe, J. R. Microsc. Soc. **1**, 388 (1881).
[44]E. Abbe, J. R. Microsc. Soc. **3**, 790 (1883).
[45]J. Y. Mutus, L. Livadaru, R. Urban, J. Pitters, A. P. Legg, M. H. Salomons, M. Cloutier, and R. A. Wolkow, New J. Phys. **15**, 073038 (2013).
[46]J. Y. Sgro, in *Virus Taxonomy: VIIIth Report of the International Committee on Taxonomy of Viruses*, 1st ed., edited by C. M. Fauquet, M. A. Mayo, J. Maniloff, U. Desselberger, and L. A. Ball (Academic Press, London, New York, 2005).
[47]F. Bawden, N. W. Pirie, J. D. Bernal, and I. Fankuchen, Nature **138**, 1051 (1936).
[48]R. E. Franklin, Biochim. Biophys. Acta **19**, 203 (1956).
[49]S. W. Smith, *The Scientist and Engineer's Guide to Digital Signal Processing* (California Technical Publication, 1997).
[50]A. Kendall, M. McDonald, and G. Stubbs, Virology **369**, 226 (2007).
[51]A. C. H. Durham, J. T. Finch, and A. Klug, Nature **229**, 37 (1971).
[52]P. J. Butler, Philos. Trans. R. Soc., B **354**, 537 (1999).
[53]J.-N. Longchamp, T. Latychevskaia, C. Escher, and H.-W. Fink, Phys. Rev. Lett. **110**, 255501 (2013).